Surface Motion and Gas Absorption

KURT MUENZ and J. M. MARCHELLO

University of Maryland, College Park, Maryland

The influence of small surface waves on mass transfer from pure gases into water has been investigated. Small amplitude progressive two-dimensional waves were mechanically generated at the liquid surface for the wave studies. Control experiments with nonwaved surfaces were also conducted. An effective diffusivity was used to correlate the data. Marked increases in mass transfer over that predicted by molecular diffusion for the no-wave control runs are attributed to natural convection motions, and are probably caused by density and surface tension variations.

Waves or ripples frequently occur at fluid-fluid interfaces (*4, 15*) and their fluid mechanical behavior has been widely studied (*19*). However, very few quantitative investigations have been made of the effect of waves on interfacial mass transfer. The objective of this study was to provide such information for small progressive two-dimensional waves with pure gas absorption into water.

This investigation deals with contact times of an hour or more. Practical application for times of this length lie mainly in the environmental area. However, methods and techniques developed may be applied to shorter contact times.

An unexpected result was encountered for the no-wave control runs. Mass transfer could not be explained simply in terms of the usual buoyant forces. It appears that even for the slightly soluble gases studied some degree of surface motion arises from Marangoni instability (*17*).

EXPERIMENTAL SYSTEMS

Oxygen, helium, carbon dioxide, and propylene were selected for the experimental work because they provide a wide range of diffusivities and solubilities. At the start of each experiment the gas under investigation was saturated to eliminate water transfer. Absorption was carried out with the use of distilled deaerated water.

The experimental procedure involved the measurement of the amount of gas absorbed as a function of time in a series of unsteady (nonflow) runs. These were carried out with no-waves and with waves of different frequencies at the surface. The unsteady state scheme was used since it required simpler experimental techniques and wave hydrodynamics than alternate steady state flow situations.

The quantity of gas absorbed as a function of time was determined by measuring the pressure, volume, and temperature of the sealed gas space. All runs were made at ambient conditions. Since water evaporation or condensation was eliminated by presaturation, the observed change in gas quantity was due to absorption alone.

The apparatus for the mass transfer studies (*11, 12*) was a sealed ripple tank (Figure 1). Waves were generated by a series of parallel vertically moving rods which could be driven at varying frequencies by a motor drive coupled to a cam mechanism. This created circular progressive wave patterns about each rod which interacted to give a two-dimensional wace front moving down the rectangularly shaped tank. Gauze enwrapped metallic screening was placed at the ends of the tank to damp out waves and prevented reflection.

The gas space gauge pressure was observed by means of a vertical U-tube mannometer whose fluid was water already saturated with the gas under investigation. A barometric reading was used along with the gauge value to obtain absolute pressure. As shown in Figure 1, equipment was provided for quantitatively decreasing gas volume as a run progressed. A series connected copper-constantan thermopile was used to measure gas temperature.

Prior to starting each run the empty ripple tank was purged for several hours with the gas to be studied. At the beginning of a run deaerated water was introduced into the tank. For the driven runs the wave generator was then turned on. Gas pressure, volume, and temperature were monitored and recorded as a function of time. Pressure was kept essentially atmospheric by incrementally decreasing gas volume in the reservoir. The P-V-T data (*11*) were used to calculate the total moles absorbed through each time interval during the run.

Kurt Muenz is with FMC Corporation, Baltimore, Maryland.

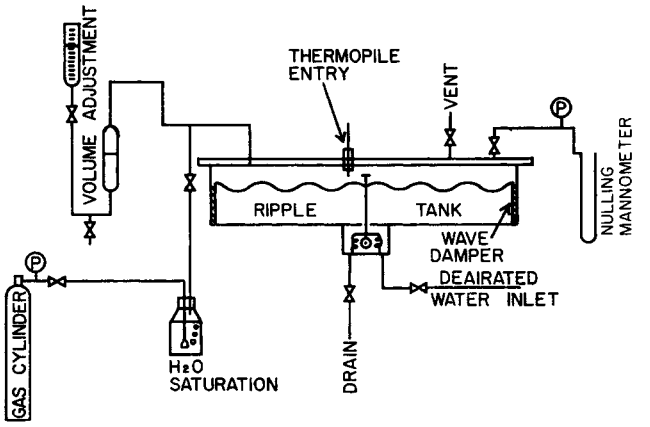

Fig. 1. Mass transfer equipment.

DATA ANALYSIS

Recognizing that the fluid motion is complex (*10, 19*), we decided (*11*) not to attempt numerical solution to the full diffusion equation. A very simple model was used to analyze the data. The model used the equation for one-dimensional unsteady diffusion into a slab with a constant diffusion coefficient.

$$\frac{\partial C}{\partial \theta} = D_w \frac{\partial^2 C}{\partial y^2} \tag{1}$$

Since the degree of agitation varies with distance from the interface, it is expected that values of D_w obtained from the data will depend not only on fluid properties, agitation intensity, and frequency, but also on fluid depth, a variable which was not studied in this work.

The boundary conditions for Equation (3) which apply to the above experiments are

$$C\,(y, 0) = 0 \tag{2}$$

$$C\,(0, \theta) = C_i \tag{3}$$

$$\partial C\,(-h, \theta)/\partial y = 0 \tag{4}$$

The series solution (*5*) to Equation (1) with these boundary conditions was integrated (*11*) to obtain the total amount of gas absorbed at any time Δn. Consideration of

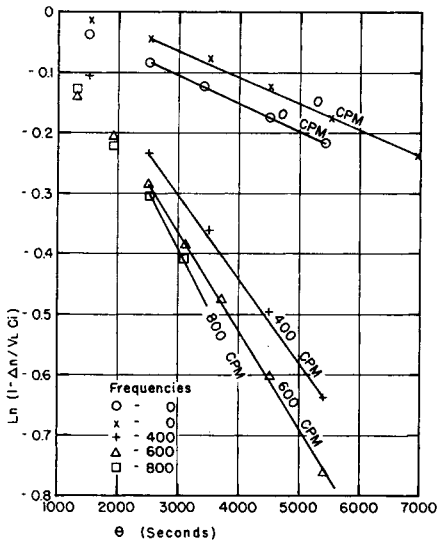

Fig. 2. Helium absorption.

the series terms indicates that for values of $D_w\pi^2\theta/4h^2 \geq 0.1$, the second term of the series is less than 5% of the first term $n = 0$. In this limit the solution may be approximated by

$$1 - (\Delta n/C_i V_L) = (8/\pi^2)\, e^{-D_w\pi^2\theta/4h^2} \qquad (5)$$

If the use of D_w as an empirical constant is justified, a plot of the experimental data in terms of $\ln(1 - \Delta n/C_i V_L)$ vs. θ should yield a straight line with a slope of $-D_w\pi^2/4h^2$. This linearity applies only for data points corresponding to times sufficiently large so that $D_w\pi^2\theta/4h^2$ is equal to or greater than 0.1.

For the case in which D_w is so small that the above criterion is not met, an alternate solution to Equation (1) may be used. For this situation it is assumed that the tank is very deep and that the boundary condition given in Equation (4) is replaced by

$$C(-\infty, \theta) = 0 \qquad (6)$$

The solution to Equation (1) with the boundary conditions of Equations (2), (3), and (6) may be integrated to obtain (12)

$$\Delta n = 2AC_i\,[(D_w\theta/\pi)^{1/2} - (D_w\theta_i/\pi)^{1/2}] \qquad (7)$$

where θ_i is an effective initial time. Equation (7) indicates that a plot of Δn vs. $\theta^{1/2}$ should give a straight line with slope equal to $2AC_i(D_w/\pi)^{1/2}$.

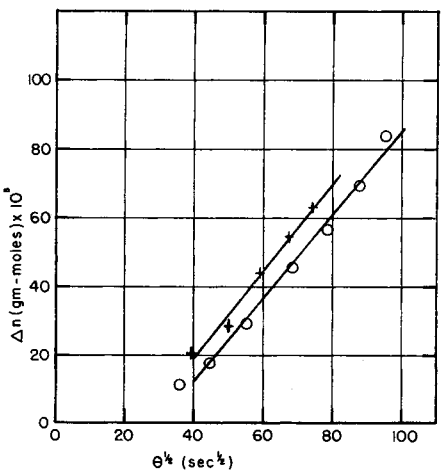

Fig. 3. Oxygen absorption with no-waves.

Equations (5) and (7) were used to correlate the experimental results in terms of an effective diffusivity. Figure 2 presents the data for the absorption of helium into water at different wave frequencies. The straight lines designate the region in which Equation (5) applies. Similar results were obtained for carbon dioxide and for the driven oxygen and propylene runs. In each of these cases for times greater than 2,400 sec. a linear relation was obtained and D_w was determined from Equation (5). For the no-wave oxygen and propylene runs the diffusivity was smaller and Equation (7) was employed. Figure 3 shows the results obtained for oxygen absorption. Values of D_w for the four gases are presented in Figure 4 as a function of wave frequency.

DISCUSSION OF NO-WAVE PHENOMENA

An appraisal of the values of D_w from Figure 4 and Table 1 indicates that for none of the gas systems do no-wave runs match predictions based on a molecular diffusion mechanism. In all cases the actual diffusivity is higher than the molecular value.

As seen in Figure 4, the propylene, oxygen, and helium systems have D_w values that increase in the order of their molecular diffusivities for a given frequency. Carbon dioxide is out of order for all frequencies, but far less so in driven runs than in no-wave runs. Figure 4 shows that a smooth extrapolation of driven values to the no-wave value can only be made for propylene. For helium and oxygen, extrapolation to zero frequency requires a sharp decrease in D_w. On the other hand, extrapolation for carbon dioxide requires an increase in D_w.

These experimental observations lead to the conclusion that the liquid phase is not motionless during no-wave runs. The reproducibility of no-wave D_w values, along with the different results for the various systems, indicates that motion is not due to random background vibrations. On the same basis it is felt that the Plexiglas walls provided adequate thermostating. It is believed that natural convection currents, dependent on the properties of the system, are present. The change in relative position of carbon dioxide for wave as opposed to no-wave runs indicates that the mechanically imposed fluid motions tend to offset or dampen these currents.

Two mechanisms for natural convection exist. The first is the familiar buoyant effect, occuring when fluid density is changed due to mass or heat transfer. A second possible mechanism is due to surface motion arising from Marangoni instability. This motion is caused by perturbations in surface concentrations which, in turn, cause changes in surface tension and hence force imbalances (17).

The Grashof number is generally used to characterize the tendency for buoyant natural convection in a system (3).

$$N_{Gr} = g\,\rho^2\,\gamma\,d^3\,\Delta z/\mu^2 \qquad (8)$$

where g is the gravity constant, d a characteristic distance (taken as the tank depth h for this case), and Δz the change in solute concentration (mole fraction) causing natural convection. The quantity γ is given by

$$\gamma = \frac{1}{\rho}\frac{d\rho}{dz} \qquad (9)$$

Since there is both a concentration and temperature effect

$$\frac{d\rho}{dz} = \left(\frac{\partial\rho}{\partial z}\right)_T + \left(\frac{\partial\rho}{\partial T}\right)_z \frac{dT}{dz} \qquad (10)$$

and

$$\frac{d\rho}{dz} = \left(\frac{\partial\rho}{\partial z}\right)_T + \left(\frac{H_s}{C_p}\right)\left(\frac{\partial\rho}{\partial T}\right) \qquad (11)$$

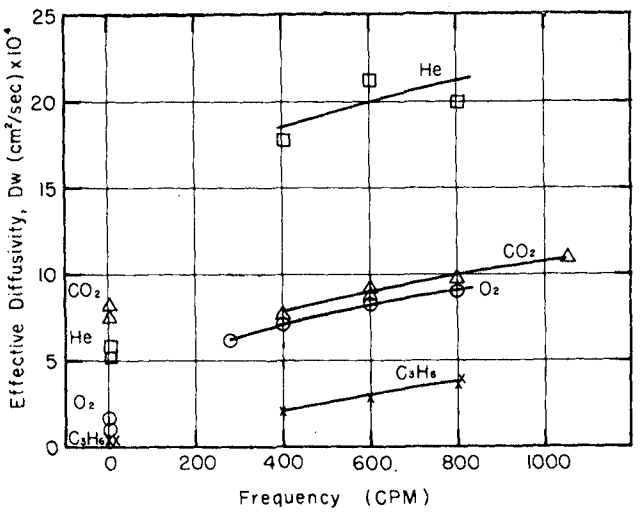

Fig. 4. Effective diffusivity for no-wave and drive runs.

C_p is the specific heat of the solution, while H_s is the heat of solution for the system and is taken as positive when heat is generated by solution. The H_s value was available for carbon dioxide; for the other systems it was estimated from equilibrium solubility data by a Clausius-Clapeyron relation (*11*). Since these are very dilute aqueous solutions, $(\partial\rho/\partial T)_z$ was determined from density vs. temperature data for water. Values for $(\partial\rho/\partial z)_T$ are not available, however. An estimate for this quantity was made by assuming ideal saturated solutions and by calculating density by the use of additive partial volumes and by linearizing the change. To estimate Grashof numbers for data correlation, saturated liquid densities were used for carbon dioxide and propylene. Since the runs were made at temperatures well above the critical point for oxygen and helium, critical densitites were used for these substances. Setting

$$\Delta z = z_s \tag{12}$$

Grashof numbers were calculated with Equations (8) through (11). These values are shown in Table 1.

In all cases, the calculations predict a decrease in density due to solution, so that negative values of Grashof number result. This indicates a condition of buoyant stability, since the density gradient that is set up is in the same direction as the gravitational field and opposite the concentration gradient.

Excluding carbon dioxide, Table 1 shows a decrease of D_w/D with increasing Grashof magnitude. This agrees with the buoyant stability concept and probably indicates that buoyant convection effects are not significant for oxygen, helium, or propylene.

Surface tension effects may, therefore, be the primary source of no-wave motion for these systems. No data on the effect of solution on surface tension for these systems were found. The estimation method described below is similar to that of Kuper and Trevens (9) and was suggested by that source.

For a pure liquid in equilibrium with its vapor, surface tension may be expressed by the McLeod equation.

Table 1. Data Correlation

Gas	D_w/D	$NGr \times 10^{-4}$	N_σ	$\partial\sigma/\partial z$	K_1
Propylene	1.77	—114.5	4.46	320	0.098
Oxygen	5.34	—11.05	—0.415	—29.9	0.150
Helium	9.85	—3.55	—2.35	—170	0.204
Carbon dioxide	44.3	—291	0.55	39.6	0.182

$$\sigma^{1/4} = (\rho_L - \rho_V)(\rho/M) \tag{13}$$

For a pure substance the Parachor may be determined from the van der Waals constants. In addition the van der Waals constants for a binary mixture can be estimated from the corresponding pure component values. In this manner a rather lengthy expression for the Parachor in terms of van der Waals constants and concentration may be obtained (*9, 11*). If the vapor density is assumed to be negligible compared to the liquid density one obtains

$$N_\sigma = 2\left[\left(\frac{a_v}{a_w}\right)^{1/2} - 1\right] + \left(\frac{7}{3}\right)\left[\frac{b_v}{b_w} - 1\right] \tag{14}$$

where

$$N_\sigma = \frac{1}{\sigma}\left(\frac{\partial\sigma}{\partial z}\right) \tag{15}$$

The subscripts v and w refer to the gas under investigation and to water, respectively. a and b are the pure-component van der Waals constants for the substance designated by the subscript.

The dimensionless group N_σ is a measure of the degree of force imbalance resulting from a surface concentration perturbation. This conclusion arises from examination of the equations governing surface tension instability and interfacial turbulence (*15, 17*). The quantity $1/\sigma$ is essentially constant for the dilute systems studied and thus $\partial\sigma/\partial z$ is the significant factor. This quantity has been used recently to correlate Marangoni behavior for liquid-liquid systems (*16*).

Values of N_σ and $\partial\sigma/\partial z$ are presented in Table 1. Negative values of N_σ indicate a decrease of surface tension as concentration increases with the reverse effect for a positive value.

WAVE EFFECTS

Experimental results clearly indicate an increase of D_w with frequency for the driven runs of all four systems. The amplitude-frequency relationship with mass transfer for these slightly soluble gases was the same as reported in reference *12*. No simple correlation was found when amplitude was used as the characteristic length. A correlation of dimensionless groups was realized by defining the group

$$F = f h^2/D \tag{16}$$

The relating equation is of the form

$$D_w/D = K_1 F^\alpha \tag{17}$$

Figure 5 is a log-log plot of D_w/D vs. F for all systems. A slope of $\alpha = 1/3$ yields a good fit to the data of the four

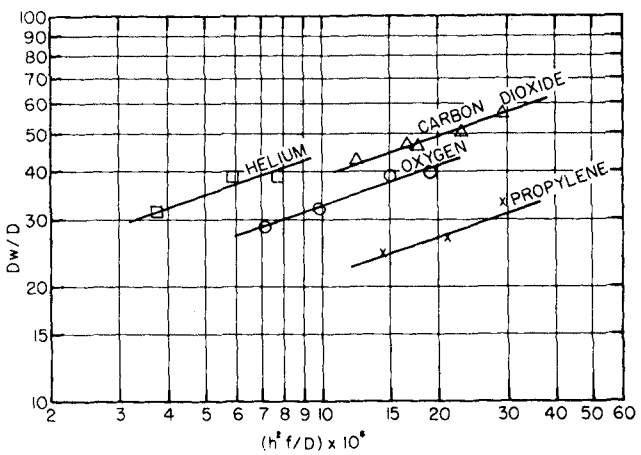

Fig. 5. Influence of frequency on effective diffusivity.

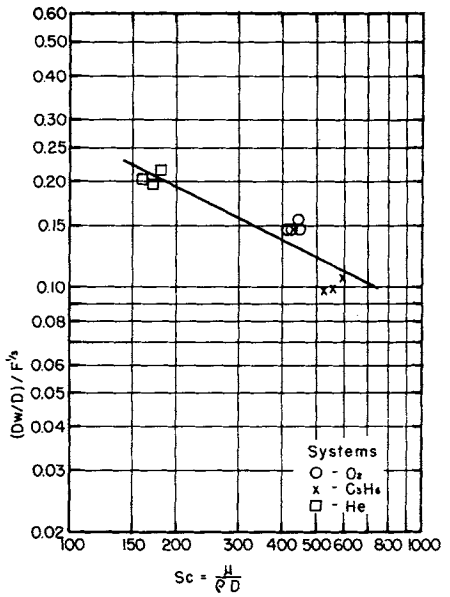

Fig. 6. Effect of molecular diffusivity.

cases. Values of K_1, determined by the intercepts of the lines, are listed in Table 1.

If carbon dioxide is excluded, a relationship of the form

$$D_w/D = K_2 N_{Sc}^{\beta} F^{1/3} \tag{18}$$

is suggested where N_{Sc} is $\mu/\rho D$. Figure 6 is a plot of $(D_w/D)/F^{1/3}$ vs. N_{Sc} for oxygen, helium, and propylene. The slope and intercept, determined by the least squares method (solid line) give values for β and K_2. Equation (18) then becomes

$$D_w/D = 2.74\, N_{Sc}^{-1/2} F^{1/3} \tag{19}$$

where the value of β actually was -0.508 but was rounded off to $-1/2$. Realizing that

$$F = \frac{fh^2}{D} = N_{Sc}\,(fh^2\rho/\mu) \tag{20}$$

one may rewrite Equation (20) as

$$D_w/D = 2.74 \left(\frac{\mu}{\rho D}\right)^{-1/6} \left(\frac{fh^2\rho}{\mu}\right)^{1/3} \tag{21}$$

The group $(fh^2\rho/\mu)$ may be thought of as a wave Reynolds number.

Two other aspects deserve comment. The first is the effect on mass transfer of the increase in surface area due to waves. This change is negligible, since amplitude to wavelength ratios were, on the average, below 0.05 (*12*). Surface area must be kept in mind, however, when working with waves of higher amplitude.

The second subject is that of turbulence. The possibility of turbulent variations to smooth particle paths exists. Such perturbations would be expected to occur in all three dimensions and surface motions in the width dimension would be expected. Another possibility is that small disturbances would prevent the paths from closing (*7*).

CONCLUSIONS

The rates of absorption of oxygen, helium, carbon dioxide, and propylene into apparently still water and by a pool in wave motion were measured. The rate of absorption followed familiar transient diffusion formulas but with effective diffusivities significantly greater than molecular values.

The production of progressive surface waves significantly increased the rate of absorption for oxygen, helium, and propylene. There is some evidence of correlation with the dimensionless groups h^2f/D and $\mu/\rho D$.

ACKNOWLEDGMENT

The authors wish to acknowledge the support of this research by the Division of Water Supply of the U. S. Department of Health, Education, and Welfare under U. S. Public Health Service Grant WP 00323.

NOTATION

A = surface area, sq. cm.
a = van der Waal constant, (atm.) (g.-mole)^2/sq. liter
a_v = van der Waal constant for gas
a_w = van der Waal constant for water
b = van der Waal constant, liter/g.-mole
b_v = van der Waal constant for gas
b_w = van der Waal constant for water
C = concentration, g.-mole/cc.
C_i = equilibrium concentration, g.-mole/cc.
C_p = specific heat, cal./g.-mole, °K.
D = molecular diffusivity, sq. cm./sec.
D_w = effective diffusivity, sq. cm.
d = characteristic system dimension, cm.
F = fh^2/D, dimensionless
f = wave frequency, sec.$^{-1}$
g = acceleration due to gravity, sq. cm./sec.
H_s = heat of solution, cal./g.-mole
h = depth of liquid, cm.
K_1 = empirical constant
K_2 = empirical constant
M = molecular weight
N_σ = $(1/\sigma)\,(\partial\sigma/\partial z)$, dimensionless
N_{Gr} = dimensionless Grashof number
N_{Sc} = Schmidt number
Δn = total gas absorbed, g.-mole
n = index for summation
P = Parachor
P- = pressure, atm.
T = absolute temperature, °K.
u = x direction velocity, cm./sec.
V = gas volume, cc.
V_L = liquid volume, cc.
v = y direction velocity, cm./sec.
x = horizontal Cartesian coordinate distance, cm.
y = vertical Cartesian coordinate distance, cm.
z = mole fraction

Greek Letters

α = empirical exponent
β = empirical exponent
γ = $(/\rho)\,(d\rho/dz)$, dimensionless
θ = time, sec.
μ = viscosity, g./(cm.) (sec.)
ρ = density, g./cc.
ρ_L = liquid density, g./cc.
ρ_v = gas density, g./cc.
σ = surface tension, dyne/cm.

LITERATURE CITED

1. Azarnoosh, Azapoor, M.S. thesis, Univ. Texas, Austin (1958).
2. Bird, R. B., "Advances in Chemical Engineering," Vol. I, p. 175, Academic Press, New York (1956).
3. ———, W. E. Stewart, and E. H. Lightfoot, "Transport Phenomena," p. 580, Wiley, New York (1960).
4. Bond, James, and M. D. Donald, *Chem. Eng. Sci.*, **6**, 237 (1957).
5. Carslaw, H. S., and J. C. Jaegar, "Conduction of Heat in Solids," 2 ed., p. 100, Oxford Press, London (1959).

6. Coulson, C. A., "Waves," 7 ed., pp. 60-84, Interscience, New York (1955).
7. Handlos, A. E., and Thomas Baron, *A.I.Ch.E. J.*, 3, 127 (1957).
8. "International Critical Tables," Vol. III, p. 254, McGraw-Hill, New York (1928).
9. Kuper, C. G., and P. H. Trevens, *Phys. Soc. Proc.*, 65, 46 (1952).
10. Longuet-Higgins, M. S., *Roy. Soc. London Phil. Trans.*, 245, 535 (1953).
11. Muenz, Kurt, Ph.D. thesis, Univ. Maryland, College Park (1965).
12. ———, and J. M. Marchello, *Rev. Sci. Inst.*, 35, 953 (1964).
13. Schlichting, Hermann, "Boundary Layer Theory," p. 461, McGraw-Hill, New York (1950).
14. Scriven, L. E., *Chem. Eng. Sci.*, 12, 98 (1960).
15. ———, and R. L. Pigford, *A.I.Ch.E. J.*, 4, 439 (1958).
16. Shain, S. A., and J. M. Prausnitz, *ibid.*, 10, 766 (1964).
17. Sternling, C. V., and L. E. Scriven, *ibid.*, 5, 514 (1959).
18. Vivian, J. E., and C. J. King, *ibid.*, 10, 520 (1964).
19. Wehausen, J. V., and E. V. Laitone, "Encyclopedia of Physics," Vol. XX, Springer Verlag, Berlin (1960).

Manuscript received January 27, 1965; revision received September 20, 1965; paper accepted September 20, 1965.

Bubble Motion and Mass Transfer in Non-Newtonian Fluids

STANLEY M. BARNETT, ARTHUR E. HUMPHREY and MITCHELL LITT

University of Pennsylvania, Philadelphia, Pennsylvania

Instantaneous mass transfer coefficients were obtained for the absorption of carbon dioxide bubbles rising in an aqueous solution of sodium carboxymethylcellulose. The rheological character of the solutions was well described by the Ellis model.

Mass transfer coefficients were high initially but trailed off rapidly with bubble age. Exceptions were found at specific diameters where the bubble shape went through a transition. At about 0.2 cm. a transition from ellipsoidal to a sphere shape occurred, which has also been observed in Newtonian fluids. At a larger diameter, however, the non-Newtonian fluid showed a shape change from a spherical "cap" to a "top" shape and finally to an ellipsoid. A sudden increase of mass transfer coefficient accompanied each shape transition.

Drag coefficient data were correlated successfully with a new Reynolds number. The Newtonian and power law portion of the Ellis model each contributed a component to the Reynolds number, which, when added together, correlated drag data for the bubbles as well as for glass spheres.

Attempts to account for transition shape changes and bubble tailing in the non-Newtonian fluid and their effects on bubble mass transfer are included.

This paper covers mass transfer from gas bubbles into a non-Newtonian fluid. Since mass transfer is directly affected by the state of the flow field, for an adequate understanding of the entire operation, it is also necessary to describe the flow conditions. Very little information is presently available. Only recently have theoretical studies of the flow of non-Newtonian fluids over solid spheres (*1, 2*) been published, while even less work has been done on liquid drops, and nothing on gas bubbles. Some results on bubble mechanics and drag in non-Newtonian fluids are also included, since they may provide an insight into the mass transfer phenomena.

Many investigators have studied mass transfer from bubbles in Newtonian systems. For practical reasons most of these studies have concerned themselves with multibubble systems. Those who did work with single bubbles generally obtained their data averaged over the life of a bubble (*3, 4*). In most cases (*5* to *7*), the results were influenced by the wake of a preceding bubble.

Many authors have studied bubble shapes (*8* to *12*). Miyagi (*13*), in particular, provided an excellent study of the shapes and oscillations during a bubble's rise. A comprehensive literature survey may be found in reference *14*.

Deindoerfer and Humphrey (*15*) obtained instantaneous mass transfer coefficients, velocities, and diameters for a bubble rising alone in distilled water. Mundkur (*16*) expanded the range of these data. The technique of Deindoerfer and Humphrey has been criticized in a recent paper by Calderbank and Lochiel (*25*), because bubble volumes and transfer rates were evaluated from projected bubble images and assumed bubble shapes. Calderbank and Lochiel also explained the fact that their data, obtained from a pressure measurement technique, is higher than Humphrey and Deindoerfer's, because the latter may have introduced impurities through the use of a plastic column. This is inferred from the fact that transfer rates decayed most rapidly soon after release, when one would expect the rate of diffusion of impurity to the surface to be highest. It is felt that the latter phenomenon was due not to impurities, but to imperfections in the bubble release mechanism, which allowed wild oscillations of the bubble upon release, giving too high a transfer rate at the outset which quickly decayed to a low value when the